

# Fluctuation-induced hopping and spin-polaron transport

L. G. L. Wegener and P. B. Littlewood

*TCM, Cavendish Laboratory, Cambridge University, Madingley Road, Cambridge, CB3 0HE, United Kingdom*

(Received 30 January 2002; published 4 December 2002)

We study the motion of free magnetic polarons in a paramagnetic background of fluctuating local moments. The polaron can tunnel only to nearby regions of local moments when these fluctuate into alignment. We propose this fluctuation-induced hopping as a transport mechanism for the spin polaron. We calculate the diffusion constant for fluctuation-induced hopping from the rate at which local moments fluctuate into alignment. The electrical resistivity is then obtained via the Einstein relation. We suggest that the proposed transport mechanism is relevant in the high-temperature phase of the Mn pyrochlore “colossal magnetoresistance” compounds and  $\text{EuB}_6$ .

DOI: 10.1103/PhysRevB.66.224402

PACS number(s): 72.20.Ee, 72.80.Ga

## I. INTRODUCTION

Recently free magnetic polarons (FMP's) have received renewed attention. They were proposed to explain the colossal magnetoresistance (CMR) in the manganese pyrochlore compounds<sup>1–6</sup> and they have been studied in the context of the double exchange model and the manganese perovskite CMR compounds.<sup>7–9</sup> Moreover, Raman-scattering data has suggested<sup>10,11</sup> that they exist in  $\text{EuB}_6$ . Previous theoretical studies have focused on the static properties of the FMP's. Here we focus on the dynamic aspect, propose a transport mechanism for an FMP, and calculate the resulting resistivity.

A magnetic polaron is a composite object consisting of a localized charge carrier and the alignment it induces in a background of local moments. Localization can occur for two different reasons: the carrier can be trapped by an impurity atom and then induce a magnetization in the region where it is localized. The resulting particle is called a “bound magnetic polaron” (BMP). It is well documented experimentally, for example, in dilute magnetic semiconductors such as  $\text{Cd}_{1-x}\text{Mn}_x\text{Se}$ ,<sup>12</sup> and in rare-earth chalcogenides.<sup>13</sup> It has been studied in depth theoretically.<sup>14</sup> A BMP is not free to roam through the sample since it is bound to its impurity. Only activated transport is possible: when the BMP is “ionized” the carrier is free to move until it is trapped by the next impurity.

However, for large enough coupling to the local moments the carrier can self-trap without the need for an impurity,<sup>15–17</sup> forming a FMP. Due to the coupling the carrier acts as a magnetic field on the local moments. The strength of this field varies in space as the probability density of the carrier: the more localized the carrier the stronger the field and the larger the energy gain resulting from aligning the local moments. The region of aligned moments therefore acts as a potential well that localizes the electron and an FMP is formed. The balance between the gain in magnetic energy from induced alignment and the loss in kinetic energy because of localization determines the polaron size. The existence of an FMP has not been conclusively established, but it has been suggested to exist both in the Mn pyrochlores<sup>4–6,18</sup> and in  $\text{EuB}_6$ .<sup>10</sup>

The mechanism of transport by FMPs is in doubt. The

conventional view is that transport is necessarily activated, as for a BMP. Here we present an alternative viewpoint: we propose that, unlike the BMP, the FMP can move between nearby sites without thermal assistance. We consider a fluctuating, paramagnetic background of local moments. A neighboring region of local moments can fluctuate into the same alignment as the polaronic moments. At that moment, the carrier can tunnel to the newly aligned region without needing to overcome an energy barrier. The tunneling process is fast compared to the spin fluctuations. After the tunneling process the carrier and the alignment have moved so that the complete FMP has hopped to the new location. The entire time evolution of the polaron formation and hopping process is illustrated in Fig. 1. We call this transport mechanism “fluctuation-induced hopping” (FIH). It does not involve an activated process. We calculate the resistivity FIH gives rise to, and find that the resistivity, though large, has a “metallic”  $T$  dependence, namely  $\partial\rho/\partial T > 0$ , in contrast to an activated process. This may help to reconcile spectroscopic evidence for FMP's (e.g., in  $\text{EuB}_6$ ) with the measured resistivity. While these ideas have not, to our knowledge, been applied in the context of spin systems, some of their counterparts in the electron-phonon problem are used in the nonadiabatic theory of superconductivity.<sup>19</sup> However, in this

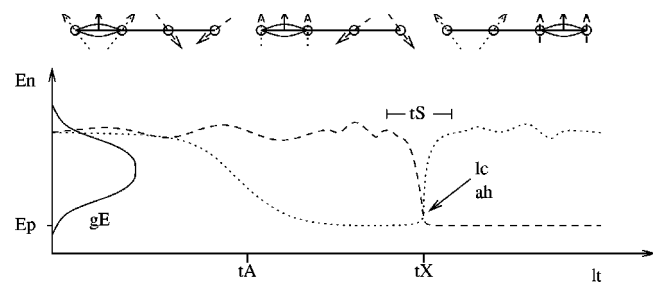


FIG. 1. Time evolution of the electron state. Solid curved lines and arrows in the upper part represent the electron density and spin. A carrier is placed on the “dotted” level. On a time scale  $\tau_A$  the carrier aligns the two moments and forms a bound small polaron. On a longer time scale  $\tau_X$ , neighboring spins (dashed line) fluctuate into alignment, which allows the carrier to tunnel into this state as the levels cross. The resonance persists for a time  $\tau_S \leq \tau_X$ . The density of states  $g(E)$  is shown on the left-hand side of the lower part.

context the emphasis lies on corrections to the electron-phonon vertex and delocalized carriers, rather than on the equivalent of the transport mechanism we propose. Related charge-transfer mechanisms have been suggested in the context of high- $T_c$  superconductivity<sup>20</sup>.

In the next section we present a model Hamiltonian that provides the frame of reference for our work. We describe the static properties of the FMP and the band states in Sec. II, postponing a justification until Appendices A and B. In Sec. III we calculate the electrical resistivity for polaron hopping. We determine the rate at which nearby regions of local moments accidentally align themselves due to fluctuations. Since the FMP tunnels to these regions, this rate determines the diffusion constant and hence the electrical resistivity.

## II. MODEL HAMILTONIAN

We consider a low-density electron gas that is coupled ferromagnetically to a background of local moments. The local moments are themselves coupled ferromagnetically. The following Hamiltonian describes this system:<sup>1,2</sup>

$$H = -t \sum_{\langle i,j \rangle \sigma} c_{i\sigma}^\dagger c_{j\sigma} - J' \sum_i \vec{\sigma}_i \cdot \vec{S}_i - J \sum_{\langle i,j \rangle} \vec{S}_i \cdot \vec{S}_j. \quad (1)$$

Here  $i$  denotes the lattice site,  $c_{i\sigma}^\dagger$  creates a conduction electron,  $\vec{S}_i$  is the local moment on site  $i$  and  $\vec{\sigma}_i$  is the conduction electron's spin.  $\langle i,j \rangle$  denotes a summation over nearest neighbors. The first term of the Hamiltonian in Eq. (1) is the kinetic energy of the carriers, and the second term couples the carriers to the local moments on which they reside. The third term couples the local moments ferromagnetically. This term can be due to, for example, superexchange. We have an  $s$ - $d$  Hamiltonian with an additional Heisenberg term. We consider the strong-coupling regime in which

$$J' \geq t \sim 10J \sim 0.1 \text{ eV}. \quad (2)$$

In our calculations we use the values  $J' = 5t$  and  $J = 0.01 \text{ eV}$  which are in agreement with experimental values in the relevant materials.<sup>1,10</sup> It should be noted that the magnetic transition is not driven by the  $s$ - $d$  part of the Hamiltonian, but only by the superexchange because of the low carrier density.

## III. POLARON AND BAND STATE

Here we present the wave function we use to study the transport properties of the FMP. Our variational calculation in Appendix A shows that the FMP is small in the strong-coupling regime: the carrier occupies approximately two lattice sites (see Fig. 3 below). We therefore use the following wave function to describe the polaron:

$$|P\rangle = \frac{1}{\sqrt{2}} (c_0^\dagger + c_1^\dagger) |0\rangle \otimes |\uparrow\rangle_{\vec{m}} \otimes |\vec{m}\rangle, \quad (3)$$

where  $\vec{S}_i$  are the polaronic local moments and  $\vec{m} = \vec{S}_0 + \vec{S}_1$  is the magnetization of the FMP. It describes a carrier localized on two lattice sites, with its spin quantized and pointing

“up” along the direction of  $\vec{m}$  to minimize the  $s$ - $d$  energy. The  $s$ - $d$  term in the Hamiltonian therefore reduces to  $-J'\sigma m$ , which is lower for more aligned local moments. This means that the carrier introduces an additional coupling between the polaronic moments. The value of the effective coupling constant can be obtained by expanding the expression for  $m$  up to first order in  $\vec{S}_0 \cdot \vec{S}_1 - S^2$  for nearly aligned polaronic moments. We obtain

$$J_{\text{eff}} = \frac{J'}{\sqrt{1 + 8S(2S+1)}} + 2J. \quad (4)$$

Since  $T \ll J'$  the moments are nearly aligned, so the polaron energy is

$$E_p = -|t| - [J' \sqrt{2S(2S+1)}/2 + 2JS^2]. \quad (5)$$

In addition to the polaron state with its induced magnetization there are many more possible states for the carrier in which it does not align any local moments. These are states in the narrowed band described in Ref. 21. Since the background fluctuates, these “band states” persist at a given location only for a time comparable to the time scale of these fluctuations, which we denote  $\tau_S$ . Nevertheless, the FMP would be unstable if a significant number of lower energy band states existed, since the carrier could then tunnel to them and gain energy.

To check whether the FMP is stable we need to estimate the position of the band edge. If the polaron level lies below the band edge, band states with a lower energy are exceedingly rare, and can be neglected. If on the other hand the band edge lies below the energy of the FMP, the latter is unstable. We determine the position of the band edge as the lowest energy of a typical band state. We use a variational approach to calculate this energy (details are given in Appendix B). The size of the band state is determined by the balance of the kinetic-energy cost of localization and the gain from the  $s$ - $d$  term. The latter is very small: the carrier aligns its spin with the total magnetization of the region in which it is localized. This magnetization is due to statistical fluctuations in the paramagnetic regime, and are consequently very small. We therefore expect the kinetic term to dominate and the band state to be very large. This is confirmed by our calculation. We show that typical band states are extended over a region of roughly  $10^6$  lattice sites. Their total energy is very close to  $-6t$  [see Eq. (B3)]. Therefore the polaron level lies below the band edge in the regime we consider ( $J' \geq t$ ), and the FMP is stable. This concludes our discussion of the static properties of the FMP and the band state. In the next section we determine their dynamic properties.

## IV. FLUCTUATION-INDUCED HOPPING

In this section we consider the FIH mechanism in detail and calculate the hopping rate of the polaron and the resulting electrical resistivity. Let us examine the time evolution of a single carrier that is injected onto a lattice site in an empty system. The local moments in its vicinity cannot respond immediately to the carrier's presence, but react on a time

scale  $\tau_A$ . On time scales smaller than  $\tau_A$ , the background appears static. A completely static background would cause Anderson localization<sup>21</sup> and trap the carrier in a state in the tail of the band below the mobility edge. Although localized, the carrier has not yet induced any alignment between local moments in its vicinity; it is in one of the band states described above. Only when the moments have aligned themselves is the energy of the state greatly reduced. This means that there is a large energy barrier that prevents the carrier from making thermal hops out of the region of alignment. However, the energy of band states fluctuates because the local moments fluctuate. It can therefore cross the polaron level. At such a crossing the electron can tunnel to this level, since there is no more energy barrier to overcome. We call this tunneling process FIH. After the electron has tunneled, the entire FMP has moved: carrier and alignment have jumped to another site. We summarize the entire time evolution in Fig. 1.

The occurrences of hops are uncorrelated in time and space since the background of local moments is paramagnetic. FIH is therefore a Markoff process and the FMP executes a random walk. In an ensemble of realizations of the polaron and the background, polarons in different realizations follow different paths. The probability density function of the polaron, defined as the fraction of realizations in an ensemble that have the FMP at a specified time at a specified location, obeys the diffusion equation.<sup>22</sup> The diffusion constant in this equation characterizes the polaron transport in the long-time limit.

For a random walk in three dimensions that consists of hops of  $l$  lattice constants, occurring with a frequency  $\omega_l$ , the diffusion constant is<sup>23</sup>

$$D = \frac{1}{6} \sum_{l=1}^{\infty} (la)^2 \omega_l, \quad (6)$$

where  $a$  is the lattice constant. The resistivity from polaron transport is then obtained from the diffusion constant by means of the Einstein formula

$$\rho = (ne\mu)^{-1} = \frac{k_B T}{ne^2 D}, \quad (7)$$

where  $\mu$  is the mobility, and  $n$  the number density of polarons.

### A. Rate of level crossings

We calculate the rate at which band state levels cross the polaron level. Such a crossing occurs when the band state energy fluctuates so much that it lies at or below the polaron level. The crossing rate depends on the size of the band state: the energy gap between the FMP and band states depends on their size. In addition to this, we will see that the energy of large band states fluctuates less. First we calculate the crossing rate for small band states.

The characteristic time,  $\tau_X$ , at which the root mean square (rms) deviation of the band state energy becomes as large as the energy gap between the two levels determines

the crossing rate. Let  $E_b(t)$  and  $E_p(t)$  denote the energies of a band and a polaronic state, respectively, at time  $t$ . Then

$$\langle [E_b(\tau_X) - E_b(0)]^2 \rangle = \langle [E_p(0) - E_b(0)]^2 \rangle \quad (8)$$

determines the mean time interval between level crossings,  $\tau_X$ . Here we have neglected the variance of the polaronic exchange energy since it is very small due to the large effective coupling constant of the polaronic moments (see Appendix II). We use  $\langle \dots \rangle_J$  to denote thermal averaging for moments coupled by an exchange constant  $J$  and rewrite Eq. (8):

$$\begin{aligned} & \langle [(\vec{S}_0(\tau_X) \cdot \vec{S}_1(\tau_X) - \vec{S}_0(0) \cdot \vec{S}_1(0))_J]^2 \rangle \\ & = (\langle \vec{S}_0 \cdot \vec{S}_1 \rangle_{J_{\text{eff}}} - \langle \vec{S}_0 \cdot \vec{S}_1 \rangle_J)^2. \end{aligned} \quad (9)$$

Here the terms arise as follows: we have used the wave function from Eq. (3) to calculate the polaron energy as  $\langle P|H|P \rangle$ . The band state energy was calculated in a similar way. We used the same spatial and spin part for the carrier, but the local moments were coupled only by  $J$ . The kinetic energies cancel out from this difference, since we are comparing polaronic and band states of the same size. The right-hand side of Eq. (9) is obtained by evaluating the expectation value of the Hamiltonian with respect to the polaron state at two different times,  $t=0$  and  $\tau_X$ . Again, kinetic energies cancel out. We now also neglect the exchange energy of the band state compared to the polaron exchange energy:

$$\langle [\vec{S}_0(\tau_X) \cdot \vec{S}_1(\tau_X)] [\vec{S}_0 \cdot \vec{S}_1] \rangle_J = \langle [\vec{S}_0 \cdot \vec{S}_1]^2 \rangle_J - \frac{1}{2} \langle \vec{S}_0 \cdot \vec{S}_1 \rangle_{J_{\text{eff}}}^2. \quad (10)$$

Equation 10 involves the four-point correlator  $\langle [\vec{S}_0(\tau_X) \cdot \vec{S}_1(\tau_X)] [\vec{S}_0 \cdot \vec{S}_1] \rangle_J$ . Since we are interested only in determining a characteristic time scale, and not the full time dependence, we may interpolate between two simple limits. First, at time  $t=0$  the correlator reduces to  $\langle (\vec{S}_0 \cdot \vec{S}_1)^2 \rangle$ . Secondly, a pair of spins at  $t=0$  is completely uncorrelated with itself at  $t=\infty$ , so that in this limit the correlator reduces to  $\langle \vec{S}_0 \cdot \vec{S}_1 \rangle^2$ . We can therefore interpolate as follows:

$$\begin{aligned} & \langle [\vec{S}_0(t) \cdot \vec{S}_1(t)] [\vec{S}_0(0) \cdot \vec{S}_1(0)] \rangle \\ & = \langle (\vec{S}_0 \cdot \vec{S}_1)^2 \rangle - f\left(\frac{t}{\tau_S}\right) [\langle (\vec{S}_0 \cdot \vec{S}_1)^2 \rangle - \langle \vec{S}_0 \cdot \vec{S}_1 \rangle^2], \end{aligned} \quad (11)$$

where the interpolation function  $f(x)$  should vary smoothly from 0 at  $x=0$  to 1 at  $x=\infty$ . Moreover, we have written  $f(t/\tau_S)$  since the four-point correlator varies on the same time scale as the fluctuations of the background. This allows us to rewrite Eq. (10) as

$$f\left(\frac{t}{\tau_S}\right) = \frac{\frac{1}{2} \langle \vec{S}_0 \cdot \vec{S}_1 \rangle_{J_{\text{eff}}}^2}{\langle (\vec{S}_0 \cdot \vec{S}_1)^2 \rangle_J - \langle \vec{S}_0 \cdot \vec{S}_1 \rangle_J^2}. \quad (12)$$

Since  $f(x)$  is a smooth function varying between 0 and 1 that changes mostly near  $x=1$ ,  $f(1)\approx 1/2$ , and  $f'(1)\approx 1$ . We expand  $f(t/\tau_S)$  up to first order about  $t=\tau_S$ , which yields

$$\frac{\tau_X}{\tau_S} \propto \frac{\langle \vec{S}_0 \cdot \vec{S}_1 \rangle_{J_{\text{eff}}}^2}{\langle (\vec{S}_0 \cdot \vec{S}_1)^2 \rangle_J - \langle \vec{S}_0 \cdot \vec{S}_1 \rangle_J^2}. \quad (13)$$

This means that crossings occur on the time scale of the fluctuations of the Heisenberg magnet weighted by the different alignments of the polaron and the background spins. Since  $k_B T \ll J'$ , the numerator of Eq. (13) reduces to  $[S(S+1)]^2$ .

The temperature dependence of  $\tau_X$  depends on the relative magnitude of the two terms in the denominator of Eq. (13). For  $k_B T \gg \mathcal{O}(J)$  they have very similar temperature dependencies, so that

$$\tau_X = A \tau_S \frac{[S(S+1)]^2}{\langle \vec{S}_0 \cdot \vec{S}_1 \rangle_J^2}, \quad (14)$$

where  $A \sim \mathcal{O}(1)$ . We use the expression given in Ref. 24 in the denominator and  $\tau_S = \hbar \sqrt{\beta/J}$  (Ref. 25) to obtain

$$\tau_X = A \frac{\hbar}{J} (\beta J)^{-3/2}. \quad (15)$$

$\tau_X$  increases with temperature. With increasing temperature level crossings become more rare. The decrease in the time scale of the spin fluctuations is more than offset by the increase of the average misalignment of the local moments.

For  $k_B T \gg J$  the temperature dependencies differ:  $\langle (\vec{S}_0 \cdot \vec{S}_1)^2 \rangle$  tends to  $S^2/3$  since the spins are completely uncorrelated, whereas  $\langle \vec{S}_0 \cdot \vec{S}_1 \rangle_J$  vanishes as  $1/T$ . Moreover the time scale of the fluctuations is different:<sup>26</sup>  $\tau_S = \hbar/\sqrt{S(S+1)J}$ . Hence  $\tau_X$  tends to a constant in this limit:

$$\tau_X = \frac{3\hbar}{J\sqrt{S(S+1)}}. \quad (16)$$

The reason is that the local moments are completely disordered in this regime; an increase in temperature does not cause an increase in disorder. The crossover between the two regimes occurs at a temperature of about  $JS(S+1)/k_B$ .

Equations (15) and (16) which are both derived from Eq. (13) in different temperature limits constitute the principal results of this section. However, before proceeding to the estimate of the diffusion constant we should check that fluctuations of other band states—in particular, those involving rearrangements of many spins—do not change our conditions. We calculate the crossing rate of large band states with the polaron level in the same way as before (see Appendix C for details). For a level crossing with a large band state, many local moments need to fluctuate into alignment simultaneously. This is a very unlikely event, and one expects the crossing rate to be accordingly small. This expectation is borne out by our calculation. In Appendix C we show that level crossings with large band states can be neglected safely.

## B. Diffusion constant

When a crossing occurs it is possible, but not necessary, for the FMP to hop. The probability,  $\mathcal{P}_l$ , of a hop of length  $l$  at a level crossing depends on the overlap between polaron and band state wave functions and on the rate at which the levels cross. The frequency at which hops of length  $l$  occur,  $\omega_l$ , is then

$$\omega_l \propto l^2 \tau_X^{-1} \mathcal{P}_l, \quad (17)$$

since the number of small band states a distance  $l$  away from the FMP is roughly proportional to  $l^2$ . The tunneling probability from the polaron state,  $|P\rangle$ , to the band state,  $|B\rangle$ , with energies  $E_P$  and  $E_B$  is given by the Zener-Landau formula<sup>27,28</sup>

$$\mathcal{P}_{P \rightarrow B} = 1 - \exp \left[ - \frac{2\pi}{\hbar} \frac{|\langle P|H|B\rangle|^2}{\left| \frac{\partial}{\partial t}(E_P - E_B) \right|} \right], \quad (18)$$

where  $H$  is the Hamiltonian for the particle. Here we have  $|\partial/\partial t(E_P - E_B)| \sim J'S/\tau_S$ , since the energy difference is due to the initially unaligned local moments in the band state. The time in which this difference between the levels disappears is  $\tau_S$ . The spatial extent of the wave functions of the polaron and the small band state limits the hopping range to one lattice constant. The overlap between neighboring small polaron states is given by

$$\langle A|H|B\rangle = \frac{1}{2} \langle 0|(c_0 + c_1)H(c_1^\dagger + c_2^\dagger)|0\rangle = -t - \frac{J'}{2}, \quad (19)$$

where the sites 0 and 1 are nearest neighbors and 1 and 2 are nearest neighbors. Therefore the hopping probability at a level crossing between two neighboring energy levels is given by

$$\mathcal{P}_{A \rightarrow B} = 1 - \exp \left\{ - 2\pi \frac{[t + J' \sqrt{2S(2S+1)/2}]^2}{JJ'} \sqrt{\frac{\beta J}{S}} \right\} \approx 1, \quad (20)$$

since  $1 \ll J'/J$ . This means also that the probability is largely independent of temperature. We will therefore take the hopping probability at a level crossing between two neighboring levels to be 1. The diffusion constant and resistivity for FIH are therefore

$$D \propto a^2 (J/\hbar) (J/k_B T)^{3/2} \quad \text{for } k_B T \gtrsim J,$$

$$D \propto a^2 (J/\hbar) / S(S+1) \quad \text{for } k_B T \gg J,$$

$$\rho \propto \frac{\hbar}{ne^2 a^2} (k_B T/J)^{5/2} \quad \text{for } k_B T \gtrsim J,$$

$$\rho \propto \frac{\hbar}{ne^2 a^2} k_B T/J \quad \text{for } k_B T \gg J. \quad (21)$$

This is our main result. We plot the resistivity versus temperature in Fig. 2 interpolating between the high- and the

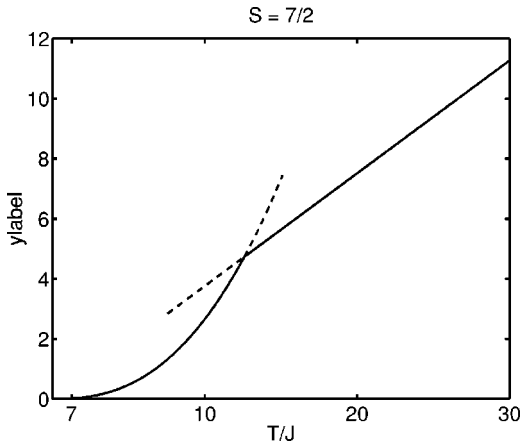


FIG. 2. Temperature dependence of the resistivity.

extremely high temperature regimes. First, the FMP can only hop to neighboring sites when a favorable statistical fluctuation aligns the local moments. These fluctuations are statistically likely in the sense that they can be estimated from the rms deviation of the spin fluctuations. Occurrences of alignment far from the polaron do not lead to hopping. Second, while small polarons typically hop by this process, large ones cannot. The required spin fluctuation into the correct configuration is statistically very rare. Third, the time scale of the spin fluctuation is slow enough that the FMP hops with probability 1 once the requisite configuration is obtained. Fourth, the diffusion constant decreases and the resistivity increases as a function of temperature. This reflects the increasing time intervals between the level crossings for higher temperatures and the relation between the resistivity and the diffusion constant.

The resistivity we obtained is “metallic:” it increases with temperature, even though we are not considering a metallic system at all. It is interesting to compare our result to the resistivity of a very dirty metal, where  $k_F \lambda_f \approx 1$ ,  $\lambda_f$  being the mean free path for the carriers. In such a material the Drude formula for the resistivity yields,

$$\rho = \frac{\hbar}{ne^2 \lambda_f^2}. \quad (22)$$

It is clear that despite its temperature dependence the polaron hopping resistivity is far too large to be confused with scattering of metallic carriers. The mean free path in the dirty metal would need to approach one lattice constant for the resistivities to be comparable. At such short mean free paths the metallic picture of delocalized carriers breaks down.

## V. CONCLUSIONS

We have proposed a transport mechanism for FMP’s in a fluctuating disordered background of local moments. In our theory the FMP hops at the occurrence of a favorable fluctuation. The transport mechanism is therefore not activated, but gives rise to a “metallic” resistivity. Experimentally our theory can be checked by a measurement of the temperature-dependent resistivity. Such measurements have been per-

formed in two systems in which the presence of a FMP has been suggested: the Mn pyrochlores and  $\text{EuB}_6$ .

In the Mn pyrochlores<sup>6,29,30</sup> the resistivity decreases with increasing temperature above  $T_c$ . This is not in accord with our predictions. There are several reasons for this. There are different types of disorder that affect the resistivity, but they were not taken into account in our work. In the In-doped compounds,<sup>29</sup> there is a miscibility gap for dopings of  $0.5 \leq x \leq 1.5$ . In this regime the bulk consists of two types of grains, each of a distinct phase with a different lattice parameter. Transport is dominated by processes associated with the grain boundaries. Phase separation is suspected to occur in the Sc-doped materials as well. A different type of disorder occurs in Bi-doped compounds: a Bi ion introduces a strong-scattering  $6s$  vacancy on the TI sublattice. This could bind the polaron, making its hopping activated. Both the scattering centers and the grain boundaries make the predicted resistivity difficult to observe.

$\text{EuB}_6$  is a much cleaner system, in which magnetic polarons have been observed by spin-flip Raman-scattering experiments.<sup>10,11</sup> There is good qualitative agreement with experiment in the high-temperature paramagnetic regime. The resistivity increases rapidly with temperature up to about 150 K and then more slowly; at temperatures above 200 K the resistivity increases even more slowly.<sup>31,32</sup> This agrees qualitatively with the crossover we predict. The crossover temperature we predict, 225 K, is only a little too large. The slow down above 200 K is probably due to other scattering mechanisms for the carriers, such as phonons, spin-orbit coupling, and scattering by carriers. There is no quantitative agreement since no  $T^{5/2}$  law is observed. This is probably due to material specific complications that our theory does not take into account:  $\text{EuB}_6$  exhibits two distinct magnetic transitions between phases with different magnetic anisotropies.<sup>32</sup>

There is good agreement as well with the two-dimensional Monte Carlo simulation.<sup>3</sup> The simulation and our work agree qualitatively on the static characteristics of the polaron, such as the temperature and  $J'$  dependence of its size and the core magnetization. We also agree on the temperature window in which the FMP exists. We do not expect more than qualitative agreement given the different parameter regimes that were explored: the simulation uses a much weaker superexchange coupling. The discrepancy between the results for the binding energy in the critical regime can be understood. The simulations show a decrease in magnitude with temperature and we predict an increase. This is due to the breakdown of our high-temperature approximation. This also explains why the simulation observes a larger polaron: we neglect the correlations between local moments except those induced by the presence of the carrier, whereas the simulation takes all correlations into account.

The dynamical simulations of FMP diffusion show qualitative departures from our results though the physical mechanisms identified for the diffusive transport are the same. In the simulations, the polaron binding energy—here again for a large polaron—decreases with temperature, and the corresponding shrinking of the polaron reduces the number of available sites for hopping. Our model is appropriate for

small polarons in a high temperature regime at least a factor of 2 above  $T_c$ .

### ACKNOWLEDGMENTS

We would like to thank Professor D. E. Khmel'nitskii, Dr. B. D. Simons, Dr. M. Côté, Dr. I. Smolyarenko, M. Calderón, M. L. Povinelli, P. Eastham, and V. Tripathi for fruitful discussions. This work was supported in part by EPSRC and Trinity College, Cambridge.

### APPENDIX A: SMALL SPIN POLARONS

We determine the size and energy of the FMP in a strong-coupling regime by a variational calculation. We choose a trial wave function for the carrier and obtain the electron density at the local moments, which acts as an external field on the moments. The resulting alignment and decrease in energy is calculated using Curie-Weiss theory. The expectation value of the energy of the trial wave function is then minimized with respect to the size of the wave function.

A Gaussian-like function is used for the electronic part of the trial wave function for the FMP; in the notation of Eq. (1):

$$|P\rangle = \frac{1}{\sqrt{\mathcal{N}}} \sum_{r_i} e^{-(r_i/\lambda)^2} c_{r_i}^\dagger |0\rangle \otimes |\uparrow\rangle_{\vec{m}} \otimes |\vec{m}\rangle, \quad (\text{A1})$$

where the vectors  $\vec{r}_i$  are the positions of the lattice sites, measured from the center of the polaron and  $\mathcal{N}$  ensures proper normalization.  $|\uparrow\rangle_{\vec{m}}$  denotes the electron spin, which is quantized and pointing “up” along the direction of the average magnetization induced by the carriers’ presence.  $|\vec{m}\rangle$  is the state vector of the polaronic local moments. The wings of this wave function take into account that a trapped electron can nearly always make short excursions to a neighboring nonpolaronic local moment. This is possible since it has nearly always a spin component parallel to this moment. These excursions diminish the polaron energy insofar as they reduce the magnetization of the core through a reduced electron density.

The magnetization of the background resulting from the presence of the carrier is obtained from Curie-Weiss theory:

$$m(\vec{r}) = \frac{3}{2} B_{3/2} \left[ \beta \left( Jm + \frac{J'}{2} \rho_{r_i} \right) \right], \quad (\text{A2})$$

where  $B$  is the Brillouin function and  $\rho_{r_i}$  is the electron density at site  $\vec{r}_i$ . Curie-Weiss theory neglects spatial correlations between the local moments that are not due to the effective field of the carrier and the induced magnetization itself. These spatial correlations are small in a paramagnet, since the coupling constant of the nonpolaronic moments is much smaller than the effective field in the core of the FMP ( $J \ll J'$ ). Curie-Weiss theory is therefore accurate in the core of the polaron. In the critical regime nonpolaronic correlations become important. Our theory is not valid there.

The expectation value of the energy of the trial wave function is minimized numerically with respect to the size,

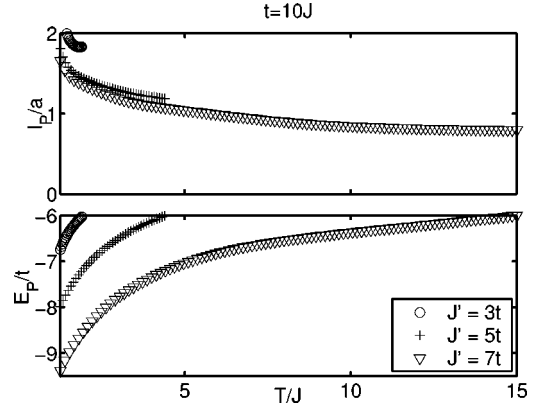


FIG. 3. Polaron size vs temperature. The curves stop when the polaron energy reaches the edge of the band (estimated in Appendix. B).

$\lambda$ , of the polaron. The results are shown below in Fig. 3. We see that the FMP is small: its size is of the order of a lattice constant over a wide range of temperatures for realistic values of the parameters. The calculated magnetization is always close to saturation in the core of the polaron, but decreases slightly as a function of temperature. For higher temperatures the FMP shrinks and its energy increases. This is because at constant size the energy gain from the  $s$ - $d$  term decreases as the temperature is raised. To compensate, the polaron shrinks, so that the effective field due to the carrier increases, which results in a magnetic energy gain. Hence, at higher temperatures, the point of minimum energy is shifted towards smaller sizes. This also means that a smaller  $s$ - $d$  coupling increases the size. The increase of the polaron energy with temperature can be understood as follows: the kinetic energy is independent of temperature and a decreasing function of size. The magnetic energy curve shifts up as temperature is raised and is an increasing function of size. Therefore, the minimum value of the total energy increases with temperature. These results are in close agreement with Ref. 1 which refers specifically to the pyrochlores.

Our calculation is well behaved at the ferromagnetic transition, even though this temperature lies outside its range of validity. As  $T_c$  is approached from above, the polaron size tends to a value of approximately  $-9.4t$  at  $T_c$ . Neither the present calculation nor Ref. 1 takes the correlations of local moments outside the FMP into account. The predicted size is therefore too small in the critical regime and the energy is overestimated.

### APPENDIX B: BAND STATES

We check whether the FMP we discovered in the previous section is bound by comparing its energy with the position of the band edge. We determine the position of the band edge as the lowest energy of typical “band states.” The energy of a band state is the difference between the energy of the system with an electron present in that state and the energy of the system in the absence of that electron. Again we use a variational approach with a trial wave function similar to Eq. (A1), with the caveat that local moments are not aligned.

Only the kinetic and the  $s$ - $d$  terms of the Hamiltonian in Eq. (1) contribute to the energy; the Heisenberg term is the same regardless of the presence of the carrier in a band state. The kinetic energy of a localized state is determined as before. The magnetic energy is estimated as follows. There is no net magnetization in the paramagnet, so the  $s$ - $d$  term in the Hamiltonian vanishes on average. In a finite region, however, there are statistical fluctuations that make it deviate from this average value, so that there is a nonzero magnetization in this region,  $\vec{m}_{\text{fluct}} = \sum_i \rho_{r_i} \vec{S}_{r_i}$ . The carrier's spin is quantized along the direction of  $\vec{m}_{\text{fluct}}$ , pointing "up." The average value of the  $s$ - $d$  term in the Hamiltonian is then

$$E_{s-d} = -\frac{J'}{2} \left\langle \sqrt{\sum_{ij} \rho_{r_i} \rho_{r_j} \vec{S}_{r_i} \cdot \vec{S}_{r_j}} \right\rangle. \quad (\text{B1})$$

The above sum is split up in one in which  $i=j$  and one in which  $i \neq j$ . We then take the thermal average of the Taylor expansion of the square root about the  $i=j$  term. The sum that contains the term with  $i \neq j$  is at least of order  $\beta J$  since it contains correlations between different local moments. The  $s$ - $d$  energy of the band state is then given by

$$E_{s-d} = -\frac{J'S}{2} \sqrt{\sum_i \rho_{r_i}^2 [1 + \mathcal{O}(\beta J)]}. \quad (\text{B2})$$

The energy of the band state is minimized numerically with respect to the size. We obtain a size of the order of  $10^6$  local moments that decreases weakly with increasing  $J'$ . We find that the  $s$ - $d$  energy is completely negligible and that the band state is so large that its energy is very close to  $-6|t|$ . We expand the band state energy to second order in  $1/l$  for large  $l$  and obtain

$$E_{\text{band}} = -6|t| \left( 1 - \frac{1}{l^2} \right) - \frac{J'S}{2} \sqrt{\frac{1}{(\sqrt{2}l)^3}}, \quad (\text{B3})$$

where  $l$  is the spatial extent of the band state. The polaron level lies therefore below the band edge and the FMP is well bound.

### APPENDIX C: CROSSING RATE WITH LARGE BAND STATES

We use the same method to calculate the crossing rate for large band states. However, instead of two spins fluctuating into nearly exact alignment, many spins need to collectively fluctuate into a more aligned configuration. The time between two crossings is again estimated from the time it takes for the rms deviation of the band state energy to become as large as the energy difference between the band level and the polaron level:

$$\langle \{E_N[\tau_X(N)] - E_N(0)\}^2 \rangle = (E_P - E_N)^2. \quad (\text{C1})$$

Here  $\tau_X(N)$  is the average time between crossings of the polaron level and a particular band state of  $N$  local moments with energy  $E_N$ . In Appendix B we calculate energy of the band state using a variational ansatz with an accurate Gauss-

ian trial wave function to show that the FMP is bound. Here, however, we determine the crossing rate and we will see that a simple model is sufficient. We assume that the carrier is localized uniformly without inducing extra alignment. Its spin is quantized along the direction of the sum of all the local moments in the band state,  $\vec{m}$ , pointing "up." The kinetic energy of the band state is approximately  $-6|t|(1 - \pi^2/N^{2/3})$  and its exchange energy vanishes on average. The kinetic energy is constant in time, so it cancels out in the left-hand side of Eq. (C1), leaving only the rms deviation of the exchange energy.

Now we use the expression for the two-site polaron of Eq. (5) on the right-hand side of Eq. (C1). The band state  $s$ - $d$  energy can be expressed as  $\sigma m(t)/N^2$  and hence Eq. (C1) becomes

$$\left[ \left\langle \left\{ \sum_{i,j,k,l}^N [\vec{S}_{r_i}^-(t) \cdot \vec{S}_{r_j}^-(t)] [\vec{S}_{r_k}^-(0) \cdot \vec{S}_{r_l}^-(0)] \right\} \right\rangle \right]_{t=0}^{t=\tau_X(N)} = 2N^2 \left[ \left( 5 - \frac{\pi^2}{N^{2/3}} \right) \frac{|t|}{J'} - \frac{S}{2} \right]^2. \quad (\text{C2})$$

The sum on the left-hand side of this equation contains  $N^2$  terms of the form  $S^4$  and  $2N$  terms of the form  $S^2 \sum_{i \neq j}^N \vec{S}_{r_i}^- \cdot \vec{S}_{r_j}^-$  where the spin operators are evaluated at equal times. There are also terms where  $i \neq j$  and  $k \neq l$ . The square root is expanded about the term of order  $N$ :

$$\begin{aligned} & \left\{ \sum_{i,j,k,l}^N [\vec{S}_{r_i}^-(t) \cdot \vec{S}_{r_j}^-(t)] [\vec{S}_{r_k}^-(0) \cdot \vec{S}_{r_l}^-(0)] \right\}^{1/2} \\ &= +NS(S+1) + \sum_{i \neq j}^N \vec{S}_{r_i}^- \cdot \vec{S}_{r_j}^- \\ &+ \sum_{i \neq j, k \neq l}^N \frac{[\vec{S}_{r_i}^-(t) \cdot \vec{S}_{r_j}^-(t)] [\vec{S}_{r_k}^-(0) \cdot \vec{S}_{r_l}^-(0)]}{2NS(S+1)} + \dots \end{aligned} \quad (\text{C3})$$

Thermal averaging both sides of this equation results in many two- and four-point spin correlators. We only retain the correlators of lowest (quadratic) order in the small parameter  $\beta J$ , thereby considering only nearest-neighbor interactions. Moreover, the first and second terms on the right-hand side of Eq. (C3) cancel in Eq. (C2) since they do not depend on time. Hence the condition for a level crossing reduces to

$$\begin{aligned} & \langle (\vec{S}_0 \cdot \vec{S}_1)^2 - \{ \vec{S}_0[\tau_X(N)] \cdot \vec{S}_1[\tau_X(N)] \} \{ \vec{S}_0 \cdot \vec{S}_1 \} \rangle \\ &= \frac{2S(S+1)N^2}{3} \left[ \left( 5 - \frac{\pi^2}{N^{2/3}} \right) \frac{|t|}{J'} - \frac{S}{2} \right]^2. \end{aligned} \quad (\text{C4})$$

The four-point correlator is treated as in Eq. (11) and we introduce the numerical constant  $A$  as in Eq. (14):

$$f(\tau_X(N)) = AN^2 \frac{2S(S+1)}{3 \langle \vec{S}_0 \cdot \vec{S}_1 \rangle^2} \left[ \left( 5 - \frac{\pi^2}{N^{2/3}} \right) \frac{|t|}{J'} - \frac{S}{2} \right]^2. \quad (\text{C5})$$

$f(t)$  could be expanded about  $t = \tau_S$  to obtain an explicit expression for  $\tau_X(N)$ . However, it is clear that large band states rarely cross the polaron level.  $f(t)$  on the left-hand side is bounded from above by 1 and the right-hand side is proportional to  $N^2$ , and so only small band states satisfy Eq. (C5). Since  $\tau_N$  grows with  $N$ , the size of the largest crossing band state follows from Eq. (C4) in the limit  $\tau_X(N) \rightarrow \infty$ . In this limit  $f(t) = 1$  so that the largest crossing band state needs  $N \sim \langle \vec{S}_0 \cdot \vec{S}_1 \rangle^2 \ll 1$ . This result shows that large band states do not cross the polaron level according to Gaussian statistics. The physical reason is that the contribution to the

$s$ - $d$  energy of a single pair of local moments is weighted by the electron density. For large states this density is low, so that alignment of a single pair of local moments does not lower the energy significantly. Thus, a crossing requires all the local moments to fluctuate into nearly perfect alignment. Of course, large clusters of ferromagnetically aligned local moments do exist, and do cross the polaron level, but they lie in the far tail of the band and are far more rare than a Gaussian approximation to the density of states would predict. These fluctuations are thus negligible. We have therefore shown that our expressions for  $\tau_X$  in Eqs. (15) and (16) give the correct hopping rate for the small FMP.

- 
- <sup>1</sup>P. Majumdar and P.B. Littlewood, Phys. Rev. Lett. **81**, 1314 (1998).  
<sup>2</sup>P. Majumdar and P.B. Littlewood, Nature (London) **395**, 479 (1998).  
<sup>3</sup>M.J. Calderón, L. Brey, and P.B. Littlewood, Phys. Rev. B **62**, 3368 (2000).  
<sup>4</sup>B. Martínez, R. Senis, J. Fontcuberta, and X. Obradors, Phys. Rev. Lett. **83**, 2022 (1999).  
<sup>5</sup>Y. Shimikawa, Y. Kubo, and T. Manako, Nature (London) **379**, 53 (1996).  
<sup>6</sup>A.P. Ramirez and M.A. Subramanian, Science **277**, 546 (1997).  
<sup>7</sup>M.Y. Kagan, D.I. Khomskii, and M.V. Mostovoy, Physica B **243**, 1209 (2000).  
<sup>8</sup>A. Moreo, S. Yunoki, and E. Dagotto, Science **283**, 2034 (1999).  
<sup>9</sup>G. Allodi, R. De Renzi, and G. Guidi, Phys. Rev. B **57**, 1024 (1998).  
<sup>10</sup>C.S. Snow, S.L. Cooper, D.P. Young, Z. Fisk, Arnaud Comment, and Jean-Philippe Ansermet, Phys. Rev. B **64**, 174412 (2001).  
<sup>11</sup>P. Nyhus, S. Yoon, M. Kaufmann, S.L. Cooper, Z. Fisk, and J. Sarrao, Phys. Rev. B **56**, 2717 (1997).  
<sup>12</sup>E.D. Isaacs, D. Heimann, M.J. Graf, B. Goldberg, R. Kershaw, D. Ridgley, K. Dwight, A. Wold, J. Furdyna, and J.S. Brooks, Phys. Rev. B **37**, 7108 (1988).  
<sup>13</sup>S. von Molnar and S. Methfessel, J. Appl. Phys. **38**, 959 (1967).  
<sup>14</sup>P. A. Wolff, in *Semiconductors and Semimetals*, edited by J. K. Furdyna and J. Kossut (Academic, New York, 1988), Vol. 25, Chap. 10.  
<sup>15</sup>T. Kasuya, A. Yanase, and T. Takeda, Solid State Commun. **8**, 1543 (1970).  
<sup>16</sup>E.L. Nagaev, Fiz. Tverd. Tela (Leningrad) **13**, 1163 (1971) [Sov. Phys. Solid State **13**, 961 (1971)].  
<sup>17</sup>C. Benoit à la Guillaume, Phys. Status Solidi B **175**, 369 (1993).  
<sup>18</sup>J.A. Alonso, P. Velasco, M.J. Martínez-Lope, M.T. Casais, J.L. Martínez, Maria T. Fernández-Díaz, and J.M. de Paoli, Appl. Phys. Lett. **76**, 3274 (2000).  
<sup>19</sup>L. Pietronero and S. Strässler, Europhys. Lett. **17**, 627 (1992).  
<sup>20</sup>A. Bill, V.Z. Kresin, and S.A. Wolf, Phys. Rev. B **57**, 10 814 (1998).  
<sup>21</sup>E.M. Kogan and M.I. Auslender, Phys. Status Solidi B **147**, 613 (1988).  
<sup>22</sup>S. Chandrasekhar, Rev. Mod. Phys. **15**, 1 (1943).  
<sup>23</sup>S. Chandrasekhar, Rev. Mod. Phys. **21**, 383 (1949).  
<sup>24</sup>S. W. Lovesey, *Condensed Matter Physics: Dynamic Correlations*, 2nd ed. (Benjamin, New York, 1986).  
<sup>25</sup>J. Hubbard, J. Phys. C **4**, 53 (1971).  
<sup>26</sup>M. Blume and J. Hubbard, Phys. Rev. B **1**, 3815 (1970).  
<sup>27</sup>C. Zener, Proc. R. Soc. London, Ser. A **137**, 696 (1932).  
<sup>28</sup>L.D. Landau, Phys. Z. Sowjetunion **1**, 426 (1932).  
<sup>29</sup>S-W. Cheong, H.Y. Hwang, B. Batlogg, and L.W. Rupp, Jr., Phys. Z. Sowjetunion **98**, 163 (1996).  
<sup>30</sup>A. Alonso, J.L. Martínez, M.J. Martínez-Lope, and M.T. Casais, Phys. Rev. Lett. **82**, 89 (1999).  
<sup>31</sup>J.C. Cooley, M. C Aronson, J.L. Sarrao, and Z. Fisk, Phys. Rev. B **56**, 14 541 (1997).  
<sup>32</sup>S. Süllow, I. Prasad, M.C. Aronson, J.L. Sarrao, Z. Fisk, D. Hristova, A.H. Lecarda, M.F. Hundley, A. Vigliante, and D. Gibbs, Phys. Rev. B **57**, 5860 (1998).